



Published in final edited form as:

Cephalalgia. 2008 September ; 28(9): 933–944. doi:10.1111/j.1468-2982.2008.01635.x.

Serotonin type 1D receptors (5HT_{1D}R) are differentially distributed in nerve fibres innervating craniofacial tissues

AM Harriott¹ and MS Gold^{2,3,4}

1 Department of Biomedical Sciences and Medical Sciences Training Program, University of Maryland, Baltimore, MD

2 Department of Medicine, Division of Gastroenterology, Hepatology and Nutrition, University of Pittsburgh, Pittsburgh, PA, USA

3 Department of Neurobiology, University of Pittsburgh, Pittsburgh, PA, USA

4 Pittsburgh Center for Pain Research, University of Pittsburgh, Pittsburgh, PA, USA

Abstract

We tested the hypothesis that the 5HT_{1D}R, the primary antinociceptive target of triptans, is differentially distributed in tissues responsible for migraine pain. The density of 5HT_{1D}R was quantified in tissues obtained from adult female rats with Western blot analysis. Receptor location was assessed with immunohistochemistry. The density of 5HT_{1D}R was significantly greater in tissues known to produce migraine-like pain (i.e. circle of Willis and dura) than in structures in which triptans have no antinociceptive efficacy (i.e. temporalis muscle). 5HT_{1D}R-like immunoreactivity was restricted to neuronal fibres, where it colocalized with calcitonin gene-related peptide and tyrosine hydroxylase immunoreactive fibres. These results are consistent with our hypothesis that the limited therapeutic profile of triptans could reflect its differential peripheral distribution and that the antinociceptive efficacy reflects inhibition of neuropeptide release from sensory afferents. An additional site of action at sympathetic efferents is also suggested.

Keywords

Headache; triptans; trigeminal ganglion neuron; sympathetic postganglionic neuron

Introduction

Triptans, serotonin type 1B/1D receptor (5HT_{1B/1D}R) agonists, are one of the most effective drugs used to treat migraine pain (1). Interestingly, the therapeutic efficacy of these compounds appears to be restricted to migraine pain. For example, in animal behavioural studies, triptans have no impact on baseline nociceptive threshold assessed with application of stimuli to somatic tissue (2) and fail to reverse sciatic nerve injury-induced decreases in paw withdrawal or vocalization thresholds (3). Similarly, naratriptan fails to attenuate noxious stimulation-evoked activity in spinal dorsal horn neurons (4). In contrast, naratriptan dose-dependently inhibited activity in trigeminal dorsal horn neurons evoked with noxious stimuli applied to the dura (4). Moreover, in clinical studies sumatriptan does not alleviate myofacial pain from temporalis muscle (5) and is of little clinical benefit to patients suffering from atypical facial pain (6). The limited therapeutic efficacy of these compounds is striking, however, in light of

evidence indicating that 5HT_{1D}R protein is present in cell bodies of both trigeminal and dorsal root ganglia (7,8).

Mechanisms underlying the therapeutic efficacy of triptans are also debated, with data in support of vasoconstriction, inhibition of neurotransmission in the central nervous system, and inhibition of peripheral neurotransmitter release from primary afferents. Initially, triptans were administered because it was thought that they could reverse the painful vasodilation associated with migraine by producing potent vasoconstriction (1). It was later discovered that the 5HT_{1B}R was responsible for this vasoconstriction, and that this receptor subtype was located postsynaptically in vascular smooth muscle (9). However, the absence of a temporal correlation between changes in vascular tone and migraine pain argues against the vascular hypothesis of triptan antinociception and for a dominant role of 5HT_{1D}R activation (10). Because the 5HT_{1D}R is expressed in primary afferent neurons and not in peripheral tissues or second-order neurons (7–9), the prevailing hypothesis is that the antinociceptive efficacy of triptans reflects the inhibition of transmitter release from primary afferents (11–14), in particular the neuropeptide calcitonin gene-related peptide (CGRP). Consistent with this hypothesis, there is evidence that triptans inhibit inflammation and CGRP release from peripheral nerve terminals (13–15). There is also evidence that triptans may reduce central neurotransmitter release primarily from afferents via a presynaptic mechanism (16).

There is general agreement that migraine pain ultimately reflects increased activity in afferents innervating the dura mater. Dural afferents have received a considerable amount of attention, given evidence that stimulation of fibres innervating the middle meningeal artery (MMA) produces pain that mimics pain felt during a migraine (17) and evidence that dural inflammation and release of CGRP from dural afferents can be blocked by sumatriptan (13,14). However, nerve fibres innervating purely vascular structures may also play a significant role in migraine pain. Stimulation of arteries proximal to the circle of Willis, such as the intracranial internal carotid arteries and middle cerebral arteries, produces migraine-like pain in neurosurgical patients (17) similar to that seen with stimulation of meningeal arteries. There are additional data to suggest that head pain can occur during carotid artery dissection, presumably via activation of trigeminovascular afferents, and that this pain may be treated with sumatriptan (18). Although there is evidence of 5HT_{1D}R in fibres innervating the dura (7,8), the presence of this receptor in other migraine-associated tissues (MATs) has yet to be investigated.

In the face of evidence suggesting that the peripheral 5HT_{1D}R contributes significantly to the therapeutic efficacy of triptans, the clinical selectivity of these drugs may be explained by differential distribution of this receptor in fibres innervating MATs vs. non-MATs. The observation that the 5HT_{1D}R is located in only 20–40% of cell bodies (8,15) is consistent with the possibility that this receptor does not have a uniform peripheral distribution. Therefore, we hypothesized that the selectivity of these drugs reflects a higher density of the 5HT_{1D}R in peripheral nerve fibres innervating MATs (common carotid artery, circle of Willis and dura mater) compared with non-migraine-associated vascular (external carotid artery) and non-vascular (temporalis muscle) tissues. To test this hypothesis, the density of 5HT_{1D}R was quantified with Western blot analysis of whole-cell lysates taken from dura, temporalis muscle, common, internal, external carotid arteries, circle of Willis and ganglia whose fibres innervate craniofacial structures. To determine where the 5HT_{1D}R was located in peripheral tissues, diaminobenzidine (DAB) immunohistochemistry of 5HT_{1D}R in whole mounted tissues from dura, extracranial and intracranial arteries was examined. Colocalization of the 5HT_{1D}R with CGRP and tyrosine hydroxylase (TH) was also examined in the dura using immunofluorescence.

Materials and methods

Animals

Adult female Sprague Dawley rats (Harlan, Indianapolis, IN, USA) weighing 150–250 g were used for all experiments. Rats were housed two per cage in the University of Pittsburgh animal facility on a 12:12 light : dark schedule with food and water freely available. Prior to all procedures, animals were deeply anaesthetized with an intraperitoneal injection (1 ml/kg) of rat cocktail containing ketamine (55 mg/kg), xylazine (5.5 mg/kg) and acepromazine (1.1 mg/kg). Experiments were approved by the University of Pittsburgh Institutional Animal Care and Use Committee and performed in accordance with National Institutes of Health guidelines for the use of laboratory animals in research.

Quantification of 5HT_{1D} R using Western blotting

The supratentorial dura mater was collected with the MMA, superior sagittal sinus and the nerves that innervate them. Additionally, the entire length of the common carotid artery was isolated from surrounding tissues by blunt dissection and separated from the accompanying jugular vein and vagus nerve. The internal, external carotid arteries and the circle of Willis were collected after these structures were dissected free from large accompanying nerves and surrounding tissues by blunt dissection. The belly of the temporalis muscle was also collected without the attached tendons. Tissues were then homogenized in RIPA buffer [50 mM Tris, 150 mM NaCl, 1 mM ethylenediamine tetraacetic acid, 1% NP 40, 0.1% sodium dodecyl sulphate (SDS)] containing protease inhibitors (6.8 µg/ml aprotinin, 4 µg/ml leupeptin, 4 µg/ml pepstatin, 4 µg/ml trypsin inhibitor, 4 µg/ml E64, 2 mM phenylmethylsulphonyl fluoride, 2 mM Na₃VO₄) on ice. Protein concentration was determined using a BioRad RCDC Protein Assay kit, and 150 µg of total protein per sample was run on 10% SDS–polyacrylamide gel electrophoresis gel. Protein was transferred to nitrocellulose membrane and blots were blocked with 5% milk and then incubated with rabbit polyclonal 5HT_{1D}R antibody (1:250; Abcam, Cambridge, MA, USA) overnight. Blots were stripped and reprobed with goat polyclonal PGP9.5 antibody (1:5000; Abcam) as a marker for neuronal tissue, mouse monoclonal β-actin (1:5000; Abcam) and mouse monoclonal glyceraldehyde 3-phosphate dehydrogenase (GAPDH) antibodies (1:5000; Abcam) as loading controls. For immunodetection, blots were incubated in peroxidase-conjugated secondary antibody (1:10 000; Jackson ImmunoResearch, West Grove, PA, USA) and visualized following chemiluminescence reaction (ECL plus; GE Healthcare, Milwaukee, WI, USA) with an LAS3000 CCD camera (FujiFilm Life Science, Stamford, CT, USA).

The band intensity from each tissue in each blot was quantified using MultiGauge software (FujiFilm Life Science). Intensities for 5HT_{1D}R immunoreactive bands were normalized either to β-actin or to PGP9.5 (as an estimate of 5HT_{1D}R relative to innervation density). Since comparisons were made between blots, these ratios were also normalized to that for a tissue common to each blot (i.e. dura or internal carotid artery). Data were expressed as the mean ± S.E.M. of the relative ratios.

Controls for Western blots

To determine the extent of non-specific binding of the primary antibody, the 5HT_{1D}R antibody was preincubated with peptide fragments corresponding to amino acids 1–18 and 251–267 of the rat 5HT_{1D}R (GenScript, Scotch Plains, NJ, USA) at a concentration of 20 µg/ml. To determine if there was non-specific binding of the secondary antibody, the primary antibody was omitted from Western blots.

Localization of 5HT_{1D}R in peripheral tissue Immunohistochemistry

Rats were transcidentally perfused with ice-cold 1× phosphate-buffered saline (pH 7.2) and ice-cold 4% paraformaldehyde. Tissues were post-fixed with 4% paraformaldehyde from 1 to 12 h. For DAB immunoperoxidase immunohistochemistry, free-floating tissues were incubated in 0.3% peroxide for 30 min, blocked with 2% normal goat serum at room temperature and then incubated in rabbit polyclonal 5HT_{1D}R primary antibody (1:500; Abcam) at 4°C for 3 days. Tissues were incubated with biotinylated goat antirabbit IgG (1:200; Vector Laboratories Vectastain kit, Burlingame, CA, USA) for 2 h at room temperature and avidin–biotin–peroxidase complex (Vector Laboratories Vectastain kit) for 30 min at room temperature. DAB (1 mg/ml with 2.5% nickel sulphate) was used to visualize 5HT_{1D}R like immunoreactive (5HT_{1D}R LI) fibres. Tissues were mounted on slides and, following ethanol dehydration, cover-slipped with Permout media (Fisher Scientific, Waltham, MA, USA).

For immunofluorescence staining of whole mounts, free-floating tissues were blocked with 10% normal donkey serum at room temperature for 1 h and then incubated in a combination of rabbit polyclonal 5HT_{1D}R (1:250; Abcam) and sheep polyclonal CGRP (1:500; Abcam) or sheep TH antibodies (1:500; Chemicon International, Temecula, CA, USA) for 48–72 h at room temperature. Free-floating tissues were then incubated in donkey antirabbit Cy3 (1:200; Jackson ImmunoResearch) and donkey antisheep Cy2 (1:500; Jackson ImmunoResearch)-conjugated secondary antibodies at room temperature for 2 h.

Superior cervical and trigeminal ganglia were removed from animals following perfusion fixation, and tissues were submerged in 30% sucrose overnight, frozen in OCT (Tissue Tek, Torrance, CA, USA) and cut in 16- μ m sections. Sectioned tissues were blocked with 5% normal donkey serum, incubated in 5HT_{1D}R (1:250), CGRP (1:500) or TH (1:500) antibody overnight at room temperature and then in donkey antirabbit or sheep Cy2 (1:200; Jackson ImmunoResearch)-conjugated secondary antibody for 2 h at room temperature.

For retrograde labelling of trigeminal ganglion neurons innervating the dura, a craniotomy was made in the area overlying the superior sagittal sinus, leaving the underlying dura intact and exposed for application of retrograde tracer 1,1'-dioctadecyl-3,3',3'-tetramethylindocarbocyanine perchloride (DiI; 170 mg/ml in dimethylsulphoxide diluted 1:10 in saline). A single droplet of DiI was applied onto the exposed dura using a 30-G needle attached to a Hamilton syringe by catheter tubing. A dental rubber dam was placed on the exposed dura and secured to the cranium with superglue adhesive. An acrylic cap made from dental orthodontic resin was used to replace the removed cranium and the incision closed with sutures. Animals received intramuscular injections of penicillin G (100 000 U/kg) and buprenorphine (0.03 mg/kg) following surgery. Ten days following application of DiI, animals were sacrificed.

Immunofluorescence staining was visualized on a Leica DM4000B (Bannockburn, IL, USA) microscope and images captured using a Leica DFC300 FX camera. Nerve fibres and cell bodies were considered immunoreactive when the immunofluorescent signal was clearly greater than that obtained when the primary antibody was omitted. For counts of 5HT_{1D}R immunoreactive cell bodies from superior cervical ganglia, three sections were examined per animal of tissue obtained from two animals. Data were expressed as the percentage of total cell bodies showing 5HT_{1D}R immunoreactivity per section in a field under $\times 200$ magnification and the average percentage was generated for each animal.

Statistical analysis

One-way analysis of variance (ANOVA) was used to assess differences between tissues. Tukey or Dunn's tests were used for post-hoc comparisons between these groups. For comparisons

between relative ratios taken from Western blots run for superior cervical and trigeminal ganglia, a *t*-test was performed. $P \leq 0.05$ was considered to be statistically significant.

Results

The density of 5HT_{1D}R LI does not vary among migraine-associated tissues

To determine if there are differences between MATs with respect to the distribution of 5HT_{1D}R protein, Western blots of whole-cell lysates from dura, common carotid artery and circle of Willis were analysed. Total protein concentration was quantified from each sample, and the same amount of protein (150 µg) was loaded per lane (Fig. 1A). Densitometric analysis of blots from eight animals, normalized to the internal carotid artery, revealed no statistically significant difference ($P > 0.05$) in the amount of 5HT_{1D}R LI between MATs (Fig. 1B). Use of β-actin as a loading control (Fig. 1A,C) confirmed that this was not due to differences in loading or transfer of proteins.

Data from previous studies suggest that the 5HT_{1D}R is present only in neural tissue (7–9). There is also evidence of differences between target tissues with respect to density of innervation (19,20). Therefore, we sought to assess the density of 5HT_{1D}R LI among MATs after taking into account differences in innervation density. The neural marker PGP9.5 was used to assess innervation density (Fig. 1A). Among MATs, there was a significantly greater amount ($P < 0.05$, $n = 8$) of PGP9.5 in circle of Willis compared with dura (Fig. 1D). However, when normalized to PGP9.5, there still remained no significant difference between MATs with respect to the 5HT_{1D}R : PGP9.5 ratio ($P > 0.05$, $n = 8$, Fig. 1E).

The density of 5HT_{1D}R is greater in MATs than in non-MATs

Since we were able to quantify 5HT_{1D}R LI in MATs, we then asked if the clinical selectivity of triptan therapy could reflect differences in the density of 5HT_{1D}R between MATs and non-MATs. The external carotid artery was used as a vascular non-MAT and the temporalis muscle was used as a non-vascular non-MAT. One-way ANOVA of the dataset, including non-MATs, indicated a significant ($P < 0.05$) effect of target tissue. Post-hoc analysis revealed that the significant effect of target tissue on 5HT_{1D}R LI was due to a significantly lower level of 5HT_{1D}R LI in external carotid artery compared with common carotid artery and circle of Willis, and a significantly lower level of 5HT_{1D}R LI in temporalis muscle compared with common carotid artery, circle of Willis and dura ($P < 0.05$, $n = 8$, Fig. 1B). The significant differences between external carotid artery, common carotid artery and circle of Willis remained when data were normalized to β-actin (Fig. 1C). Because β-actin was undetectable in striated muscle (Fig. 1A), GAPDH was used as a loading control (data not shown). The relatively high level of GAPDH in striated muscle highlights difficulties associated with assessing relative protein levels between distinct tissue types, but argues against the suggestion that the relatively low density of 5HT_{1D}R LI detected in muscle was due to problems with loading or transfer of proteins.

One-way ANOVA of the dataset, including non-MATs, again revealed a significant ($P < 0.05$) effect of target tissue with respect to levels of PGP9.5 LI. Post-hoc analysis indicated the density of PGP9.5 in temporalis muscle was significantly ($P < 0.05$) greater than that in dura (Fig. 1D). Pooled data from eight animals indicated that the relative density of 5HT_{1D}R LI normalized to PGP9.5 in the external carotid artery was significantly lower than that in the common carotid artery and circle of Willis ($P < 0.05$; Fig. 1E). Likewise, the density of 5HT_{1D}R LI in temporalis muscle was significantly lower than that in the common carotid artery, circle of Willis or dura ($P < 0.05$; Fig. 1E).

Pre-absorption of the 5HT_{1D}R antibody with the peptide it was raised against was used to confirm the specificity of the immunoreactivity. This eliminated the two bands present in all tissues (approximately 60 and 62 kDa) and the high-molecular-weight band (approximately 65 kDa) restricted to the dura (control: Fig. 1A). Similar results were obtained following omission of the primary antibody (data not shown).

5HT_{1D}R LI is primarily localized to neuronal fibres innervating peripheral tissues

To confirm that 5HT_{1D}R LI detected with Western blot analysis was associated with neural tissue, localization of the receptor was assessed with immunohistochemistry. We observed 5HT_{1D}R LI in nerve fibres innervating the rat dura mater. There did not appear to be any 5HT_{1D}R LI in the meningeal arteries or resident mast cells. 5HT_{1D}R LI fibres of the dura mater ran along with the MMA. These fibres branched with arterial bifurcations. There were also 5HT_{1D}R LI fibres that intersected the MMA and traversed the meninges in a direction perpendicular to the MMA and parallel to the superior sagittal sinus (Fig. 2A). 5HT_{1D}R LI was present in large nerve trunks and smaller fibres (Fig. 2B). In addition, we observed 5HT_{1D}R LI nerve fibres in segments of the extracranial and intracranial cerebrovasculature, including the external carotid artery and circle of Willis (Fig. 2C,D, respectively).

5HT_{1D}R LI is colocalized with CGRP LI in the dura mater

Given evidence of 5HT_{1D}R-mediated inhibition of CGRP release (11,14), we sought to determine the extent to which there is colocalization of the receptor with this primary afferent neuropeptide in peripheral tissue. Double-labelling experiments revealed the presence of both 5HT_{1D}R LI and CGRP LI within dural nerve bundles (Fig. 3A,B). However, there were also nerve bundles that displayed 5HT_{1D}R LI that did not overlap with CGRP LI (Fig. 3C).

Although CGRP is commonly used a marker for peptidergic sensory neurons, neuropeptide immunoreactivity, including CGRP LI, has been detected in subpopulations of sympathetic postganglionic neurons (SPGNs) (21). Therefore, in order to assess the possibility that a portion of the CGRP LI fibres innervating the dura were from SPGNs, we probed the superior cervical ganglion (SCG) for the presence of CGRP LI. Trigeminal ganglia (TG) from the same rats were collected and run in parallel as a positive control. We were unable to detect the presence of CGRP LI in SCG from two rats, despite CGRP LI in small- and medium-diameter TG neurons (Fig. 4). The absence of CGRP LI in rat SCG is consistent with previous reports indicating that although CGRP LI is present in human, feline and canine SCG, it is undetectable in SCG from rat or guinea pig (21–23).

5HT_{1D}R LI is present in sympathetic postganglionic neurons innervating the dura mater

Considering recent evidence that sympathetic activity may modulate afferent signalling in the dura mater (24) and the dense innervation of the dural parenchyma and MMA by TH LI fibres, (presumably arising from the superior cervical ganglia: Fig. 5A), we determined if the non-peptidergic 5HT_{1D}R LI fibres could be sympathetic efferent. Double-labelling experiments revealed colocalization of 5HT_{1D}R LI with TH in a number of dural fibres (Fig. 5B).

To confirm that this staining was indeed from the SCG, the presence of 5HT_{1D}R LI was assessed in SCG. Again, TG from the same rats were run in parallel (Fig. 6A). In six sections of SCG from two rats, 9% of cell bodies displayed 5HT_{1D}R LI (Fig. 6B). To assess the density of 5HT_{1D}R in SCG relative to that in TG, Western blots of whole-cell lysates generated from both tissues were processed. Pooled data from five rats normalized to PGP9.5 suggested that, on average, there is a twofold higher density of 5HT_{1D}R in the TG compared with the SCG ($P = 0.012$, Fig. 6C).

Previous reports have indicated that there is a subpopulation of sensory neurons with TH LI (25,26). Therefore, in order to determine the extent to which TH LI fibres innervating the dura could arise from the TG, we probed TG retrogradely labelled from the dura with DiI, for the presence of TH LI. Four sections each from TG obtained from two rats were analysed. TH LI was clearly detectable in a small subpopulation (3–4%) of TG neurons (Fig. 7A). However, none of the 52 TG neurons that were retrogradely labelled with DiI displayed TH LI (Fig. 7B).

Discussion

The present study was designed to test the hypothesis that the selective therapeutic efficacy of triptans reflects a high density of 5HT_{1D}R in tissues underlying migraine pain. We observed that there was no difference between MATs with respect to the relative density of 5HT_{1D}R. However, the relative density of 5HT_{1D}R was lower in non-MATs (i.e. temporalis muscle) than in MATs. 5HT_{1D}R LI was restricted to nerve fibres innervating peripheral tissues, where it was colocalized in many fibres with the neuropeptide CGRP. 5HT_{1D}R LI was also colocalized with TH in many fibres that appeared to arise from the superior cervical ganglia.

5HT_{1D}R LI is present in a number of MATs

Our conclusion that the distribution of the 5HT_{1D}R is similar between MATs is based on Western blot data showing no significant differences in the amounts of 5HT_{1D}R in the common carotid artery, circle of Willis or dura, whether data were analysed as a function of total protein, normalized to loading controls such as β -actin, or normalized to innervation density estimated with PGP9.5. To justify the normalization of 5HT_{1D}R to PGP9.5, we explored the possibility that non-neuronal components of peripheral tissues might contain the 5HT_{1D}R. Consistent with previous reports demonstrating that 5HT_{1D}R mRNA and protein are not found in intracranial arteries but rather in the perivascular nerves that innervate them (7,9), our data also indicate that 5HT_{1D}R LI is restricted to nerve fibres. It is always possible that we have overestimated density of 5HT_{1D}R in the common carotid artery and circle of Willis due to contamination with fibres of passage. However, we suggest that such an overestimation is minimal based on our anatomical results (Fig. 2), which were consistent with a terminal pattern of innervation and the observation that there is no rostral–caudal trend to the pattern of distribution (i.e. higher levels found in proximal structures such as common carotid artery and lower levels found in distal structures such as circle of Willis).

Prior studies have indicated that activation of nerve fibres innervating the dura mater plays a critical role in generating migraine pain. For example, in neurosurgical patients, stimulation of afferents innervating dural blood vessels produced migraine-like pain (17). Furthermore, inflammatory mediators released during the ictal period of migraine are able to increase activity of dural afferents and their second-order neurons in the trigeminal nucleus following exogenous application to the dura (27,28). Importantly, these inflammation-induced changes in dural afferent activity can be blocked by sumatriptan. Sumatriptan is also able to decrease plasma protein extravasation in the dura and CGRP release from dural afferents. Although little attention has been paid to other blood vessels of the head and neck and the afferents that innervate them, our results demonstrating high density of the 5HT_{1D}R in nerve fibres innervating the common carotid artery and circle of Willis suggest that other populations of vascular afferents, in addition to those innervating the dura mater, may contribute to migraine pain. This conclusion is supported by immunohistochemistry demonstrating innervation of intracranial arteries by nociceptive-like afferents containing both CGRP and substance P (29), by clinical observations that endovascular procedures resulting in the stimulation of several arteries within the cranial vault are painful (30), and early studies demonstrating that stimulation of proximal branches of the circle of Willis produces migraine-like pain (17). In addition, there are data suggesting that head pain occurs during dissection of the carotid artery,

presumably via activation of trigeminovascular afferents; and that this pain may be treated with sumatriptan (18).

The density of 5HT_{1D}R is greater in MATs than in non-MATs

Although there are few reports to suggest that triptans may inhibit peripheral inflammation irrespective of tissue type, (8,31), as summarized in the Introduction, there are a number of studies demonstrating selectivity in the antinociceptive efficacy of triptans (4–6,32). Our data indicating the density of 5HT_{1D}R is lower in temporalis muscle than common carotid artery, circle of Willis or dura are consistent with our hypothesis and suggest that the lower density of receptor in nerve fibres innervating the temporalis muscle may have contributed to failure of triptans in the clinical trial of myofascial pain arising from the temporalis muscle (5).

There may be unique processing of the 5HT_{1D}R within the dura

Interestingly, three distinct 5HT_{1D}R LI bands (56, 60 and 62 kDa) were detected in our Western blots of lysates from dura and other vascular tissues. The lower-molecular-weight band was not detected in the temporalis muscle, the TG or the SCG. An additional higher-molecular-weight band (65 kDa) was detected in the dura. All four bands were eliminated by pre-absorption of the primary antibody, suggesting the bands contain a protein with a specific 5HT_{1D}R epitope. That the 65-kDa band was absent in the trigeminal ganglion or in lysates taken from the brainstem (data not shown) argues against a splice variant, and for a post-translational modification in the peripheral target. Inspection of the 5HT_{1D}R protein sequence reveals several sites for post-translational modification, specifically, N-glycosylation (33). Thus, there may be post-translational processing of the receptor as the receptor is being trafficked or at the peripheral terminal innervating the end organ. The fact that we observed this higher-molecular-weight band only in the dura suggests an alternative mechanism for the therapeutic specificity of triptans.

5HT_{1D}R LI in peptidergic primary afferent fibres

Previous data suggest that expression of 5HT_{1D}R in the cell bodies of sensory neurons is restricted to a subpopulation of neurons expressing CGRP, with 75–90% of 5HT_{1D}R+ neurons double-labelled with CGRP (8,15,34). Consistent with these reports, we observed colocalization of 5HT_{1D}R and CGRP in dural fibres. This overlap in the periphery supports the hypothesis that triptan inhibition of peripheral CGRP release is via a direct mode of action (i.e. on the afferent terminal). However, our data also suggest 5HT_{1D}R is present in non-peptidergic fibres. At least some of these fibres appear to be SPGNs, given colocalization of 5HT_{1D}R LI with TH LI in the dura mater and the presence of 5HT_{1D}R LI in cell bodies of the SCG. That these receptors on SPGNs are functional is suggested by the observation that 5HT_{1D}R agonists inhibit sympathetically mediated pressor and tachycardic responses (35, 36).

A role for SPGNs in migraine?

The presence of 5HT_{1D}R LI in SPGNs raises the possibility that the therapeutic efficacy of triptans reflects an action of these neurons innervating the dura mater or other vascular tissues. Given the hypothesis that migraine pain may be caused by painful dilation of dural blood vessels (17), one might predict that an increase in sympathetic efferent activity would result in pain relief in association with vasoconstriction. However, there is also evidence that the SPGN may contribute to peripheral inflammation. For example, sympathetic efferents have been shown to release adenosine triphosphate (37) and prostaglandin (PG) E₂ (38), which would contribute to primary afferent activation and sensitization and therefore neurogenic inflammation and pain. Importantly, recent evidence indicates that sympathomimetics increase basal levels of PGE₂ in rat dura mater (24).

In summary, there remain a number of other possible factors that might contribute to the clinical selectivity of triptans, including potential differences in bioavailability and pharmacology of peripherally located receptors, contributions of central spinal and supraspinal receptors, and the minimum number of 5HT_{1D}R-containing fibres needed to appreciate differences in pain perception. Nevertheless, our results are consistent with the hypothesis that the therapeutic efficacy of triptans may reflect, at least in part, a selective pattern of 5HT_{1D}R expression, with the highest density of receptor in the innervation of structures likely to contribute to migraine pain. Although the location of this receptor in peptide-containing nerve fibres innervating peripheral tissues is consistent with the suggestion that pain relief reflects inhibition of CGRP release from peripheral afferent terminals, the presence of the receptor on SPGN terminals raises the possibility that the therapeutic efficacy of triptans may also reflect an action on efferent fibres. Teasing out the relative importance of these two mechanisms of action may enable the development of more selective and effective treatments for migraine.

Acknowledgements

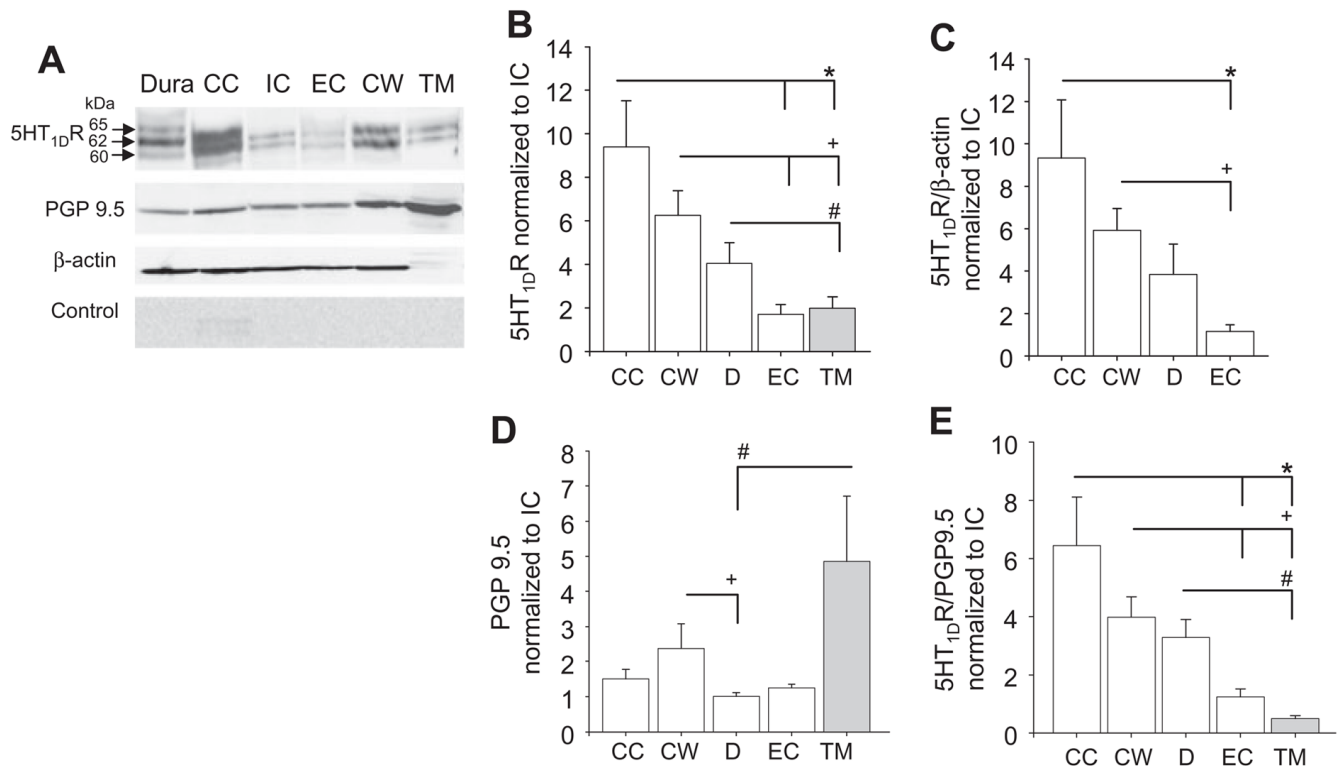
We thank Dr Andrew Ahn for helpful discussions during the design of this study and Dr H. Richard Koerber for help during the preparation of this manuscript. This work was supported by NIH grants NS059153 (A.M.H.) NS41384 (M.S.G.).

References

1. Waeber C, Moskowitz MA. Therapeutic implications of central and peripheral neurologic mechanisms in migraine. *Neurology* 2003;61:S9–20. [PubMed: 14581653]
2. Ottani A, Ferraris E, Giuliani D, Mioni C, Bertolini A, Sternieri E, Ferrari A. Effect of sumatriptan in different models of pain in rats. *Eur J Pharmacol* 2004;497:181–6. [PubMed: 15306203]
3. Kayser V, Aubel B, Hamon M, Bourgoin S. The antimigraine 5-HT 1B/1D receptor agonists, sumatriptan, zolmitriptan and dihydroergotamine, attenuate pain-related behaviour in a rat model of trigeminal neuropathic pain. *Br J Pharmacol* 2002;137:1287–97. [PubMed: 12466238]
4. Cumberbatch MJ, Hill RG, Hargreaves RJ. Differential effects of the 5HT_{1B/1D} receptor agonist naratriptan on trigeminal versus spinal nociceptive responses. *Cephalalgia* 1998;18:659–63. [PubMed: 9950621]
5. Dao TT, Lund JP, Remillard G, Lavigne GJ. Is myofascial pain of the temporal muscles relieved by oral sumatriptan? A cross-over pilot study. *Pain* 1995;62:241–4. [PubMed: 8545150]
6. Harrison SD, Balawi SA, Feinmann C, Harris M. Atypical facial pain: a double-blind placebo-controlled crossover pilot study of subcutaneous sumatriptan. *Eur Neuropsychopharmacol* 1997;7:83–8. [PubMed: 9169294]
7. Longmore J, Shaw D, Smith D, Hopkins R, McAllister G, Pickard JD, et al. Differential distribution of 5HT_{1D}- and 5HT_{1B}-immunoreactivity within the human trigemino-cerebrovascular system: implications for the discovery of new antimigraine drugs. *Cephalalgia* 1997;17:833–42. [PubMed: 9453271]
8. Potrebic S, Ahn AH, Skinner K, Fields HL, Basbaum AI. Peptidergic nociceptors of both trigeminal and dorsal root ganglia express serotonin 1D receptors: implications for the selective antimigraine action of triptans. *J Neurosci* 2003;23:10988–97. [PubMed: 14645495]
9. Bouchelet I, Cohen Z, Case B, Seguela P, Hamel E. Differential expression of sumatriptan-sensitive 5-hydroxytryptamine receptors in human trigeminal ganglia and cerebral blood vessels. *Mol Pharmacol* 1996;50:219–23. [PubMed: 8700126]
10. Olesen J, Friberg L, Olsen TS, Iversen HK, Lassen NA, Andersen AR, Karle A. Timing and topography of cerebral blood flow, aura, and headache during migraine attacks. *Ann Neurol* 1990;28:791–8. [PubMed: 2285266]
11. Durham PL, Russo AF. Regulation of calcitonin gene-related peptide secretion by a serotonergic antimigraine drug. *J Neurosci* 1999;19:3423–9. [PubMed: 10212302]

12. Goadsby PJ, Edvinsson L. The trigeminovascular system and migraine: studies characterizing cerebrovascular and neuropeptide changes seen in humans and cats. *Ann Neurol* 1993;33:48–56. [PubMed: 8388188]
13. Buzzi MG, Carter WB, Shimizu T, Heath H 3rd, Moskowitz MA. Dihydroergotamine and sumatriptan attenuate levels of CGRP in plasma in rat superior sagittal sinus during electrical stimulation of the trigeminal ganglion. *Neuropharmacology* 1991;30:1193–200. [PubMed: 1663596]
14. Limmroth V, Katsarava Z, Liedert B, Guehring H, Schmitz K, Diener HC, Michel MC. An *in vivo* rat model to study calcitonin gene related peptide release following activation of the trigeminal vascular system. *Pain* 2001;92:101–6. [PubMed: 11323131]
15. Hou M, Kanje M, Longmore J, Tajti J, Uddman R, Edvinsson L. 5-HT(1B) and 5-HT(1D) receptors in the human trigeminal ganglion: co-localization with calcitonin gene-related peptide, substance P and nitric oxide synthase. *Brain Res* 2001;909:112–20. [PubMed: 11478927]
16. Levy D, Jakubowski M, Burstein R. Disruption of communication between peripheral and central trigeminovascular neurons mediates the antimigraine action of 5HT 1B/1D receptor agonists. *Proc Natl Acad Sci USA* 2004;101:4274–9. [PubMed: 15016917]
17. Ray B, Wolff H. Experimental studies on headache. Pain-sensitive structures of the head and their significance in headache. *Arch Surg* 1940;41:813–56.
18. Leira EC, Cruz-Flores S, Leacock RO, Abdulrauf SI. Sumatriptan can alleviate headaches due to carotid artery dissection. *Headache* 2001;41:590–1. [PubMed: 11437896]
19. Perry MJ, Lawson SN. Differences in expression of oligosaccharides, neuropeptides, carbonic anhydrase and neurofilament in rat primary afferent neurons retrogradely labelled via skin, muscle or visceral nerves. *Neuroscience* 1998;85:293–310. [PubMed: 9607720]
20. Provitera V, Nolano M, Pagano A, Caporaso G, Stancanelli A, Santoro L. Myelinated nerve endings in human skin. *Muscle Nerve* 2007;35:767–75. [PubMed: 17405136]
21. Hisa Y, Koike S, Uno T, Tadaki N, Bamba H, Okamura H, et al. Coexistence of calcitonin gene-related peptide and NADPH-diaphorase in the canine superior cervical ganglion. *Neurosci Lett* 1997;228:135–8. [PubMed: 9209117]
22. Baffi J, Gorcs T, Slowik F, Horvath M, Lekka N, Pasztor E, Palkovits M. Neuropeptides in the human superior cervical ganglion. *Brain Res* 1992;570:272–8. [PubMed: 1352173]
23. Jones MA, Marfurt CF. Calcitonin gene-related peptide and corneal innervation: a developmental study in the rat. *J Comp Neurol* 1991;313:132–50. [PubMed: 1761750]
24. Ebersberger A, Takac H, Richter F, Schaible HG. Effect of sympathetic and parasympathetic mediators on the release of calcitonin gene-related peptide and prostaglandin E from rat dura mater, *in vitro*. *Cephalalgia* 2006;26:282–9. [PubMed: 16472334]
25. Vega JA, Amenta F, Hernandez LC, del Valle ME. Presence of catecholamine-related enzymes in a subpopulation of primary sensory neurons in dorsal root ganglia of the rat. *Cell Mol Biol* 1991;37:519–30. [PubMed: 1682049]
26. Brumovsky P, Villar MJ, Hokfelt T. Tyrosine hydroxylase is expressed in a subpopulation of small dorsal root ganglion neurons in the adult mouse. *Exp Neurol* 2006;200:153–65. [PubMed: 16516890]
27. Strassman AM, Raymond SA, Burstein R. Sensitization of meningeal sensory neurons and the origin of headaches. *Nature* 1996;384:560–4. [PubMed: 8955268]
28. Burstein R, Jakubowski M. Analgesic triptan action in an animal model of intracranial pain: a race against the development of central sensitization. *Ann Neurol* 2004;55:27–36. [PubMed: 14705109]
29. Zhu BS, Blessing WW, Gibbins IL. Parasympathetic innervation of cephalic arteries in rabbits: comparison with sympathetic and sensory innervation. *J Comp Neurol* 1997;389:484–95. [PubMed: 9414008]
30. Martins IP, Baeta E, Paiva T, Campos J, Gomes L. Headaches during intracranial endovascular procedures: a possible model of vascular headache. *Headache* 1993;33:227–33. [PubMed: 8320095]
31. Pierce PA, Xie GX, Peroutka SJ, Levine JD. Dual effect of the serotonin agonist, sumatriptan, on peripheral neurogenic inflammation. *Reg Anesth* 1996;21:219–25. [PubMed: 8744664]
32. Connor HE, Feniuk W, Beattie DT, North PC, Oxford AW, Saynor DA, Humphrey PP. Naratriptan: biological profile in animal models relevant to migraine. *Cephalalgia* 1997;17:145–52. [PubMed: 9170336]

33. Wurch T, Palmier C, Colpaert FC, Pauwels PJ. Sequence and functional analysis of cloned guinea pig and rat serotonin 5-HT_{1D} receptors: common pharmacological features within the 5-HT_{1D} receptor subfamily. *J Neurochem* 1997;68:410–18. [PubMed: 8978753]
34. Ma QP, Hill R, Sirinathsinghji D. Colocalization of CGRP with 5-HT_{1B/1D} receptors and substance P in trigeminal ganglion neurons in rats. *Eur J Neurosci* 2001;13:2099–104. [PubMed: 11422450]
35. Moran A, Fernandez MM, Velasco C, Martin ML, San Roman L. Characterization of prejunctional 5-HT₁ receptors that mediate the inhibition of pressor effects elicited by sympathetic stimulation in the pithed rat. *Br J Pharmacol* 1998;123:1205–13. [PubMed: 9559906]
36. Sanchez-Lopez A, Centurion D, Vazquez E, Arulmani U, Saxena PR, Villalon CM. Further characterization of the 5-HT₁ receptors mediating cardiac sympatho-inhibition in pithed rats: pharmacological correlation with the 5-HT_{1B} and 5-HT_{1D} subtypes. *Naunyn Schmiedebergs Arch Pharmacol* 2004;369:220–7. [PubMed: 14673512]
37. Green PG, Basbaum AI, Helms C, Levine JD. Purinergic regulation of bradykinin-induced plasma extravasation and adjuvant-induced arthritis in the rat. *Proc Natl Acad Sci USA* 1991;88:4162–5. [PubMed: 2034661]
38. Coderre TJ, Basbaum AI, Levine JD. Neural control of vascular permeability: interactions between primary afferents, mast cells, and sympathetic efferents. *J Neurophysiol* 1989;62:48–58. [PubMed: 2502607]

**Figure 1.**

Quantification of 5HT_{1D}R in migraine-associated tissues (MATs) and non-MATs. (A) Top panel: Western blot of total protein (150 μg/lane) from whole-cell lysates of dura (D), common (CC), internal (IC), external (EC) carotid arteries, circle of Willis (CW) and temporalis muscle (TM) probed for 5HT_{1D}R. All structures were obtained from a single rat. Middle panel: blot in A was re-probed with antibodies against PGP9.5 and β-actin. Bottom panel: Control blots were pre-incubated with the peptide used to generate the 5HT_{1D}R antibody. (B) Pooled data ($n = 8$) indicate the presence of statistically significant differences between tissues with respect to the amount of 5HT_{1D}R. (C) Significant differences between CC, CW and EC were also observed when data were normalized to β-actin. (D) There was a statistically significantly difference in the relative amount of PGP9.5 between target tissues. (E) Pooled data indicate the presence of statistically significant differences between tissues with respect to relative levels of 5HT_{1D}R normalized to PGP9.5. *Statistically significant differences from CC. +Statistically significant differences from CW. #Statistically significant differences from D where $P < 0.05$.

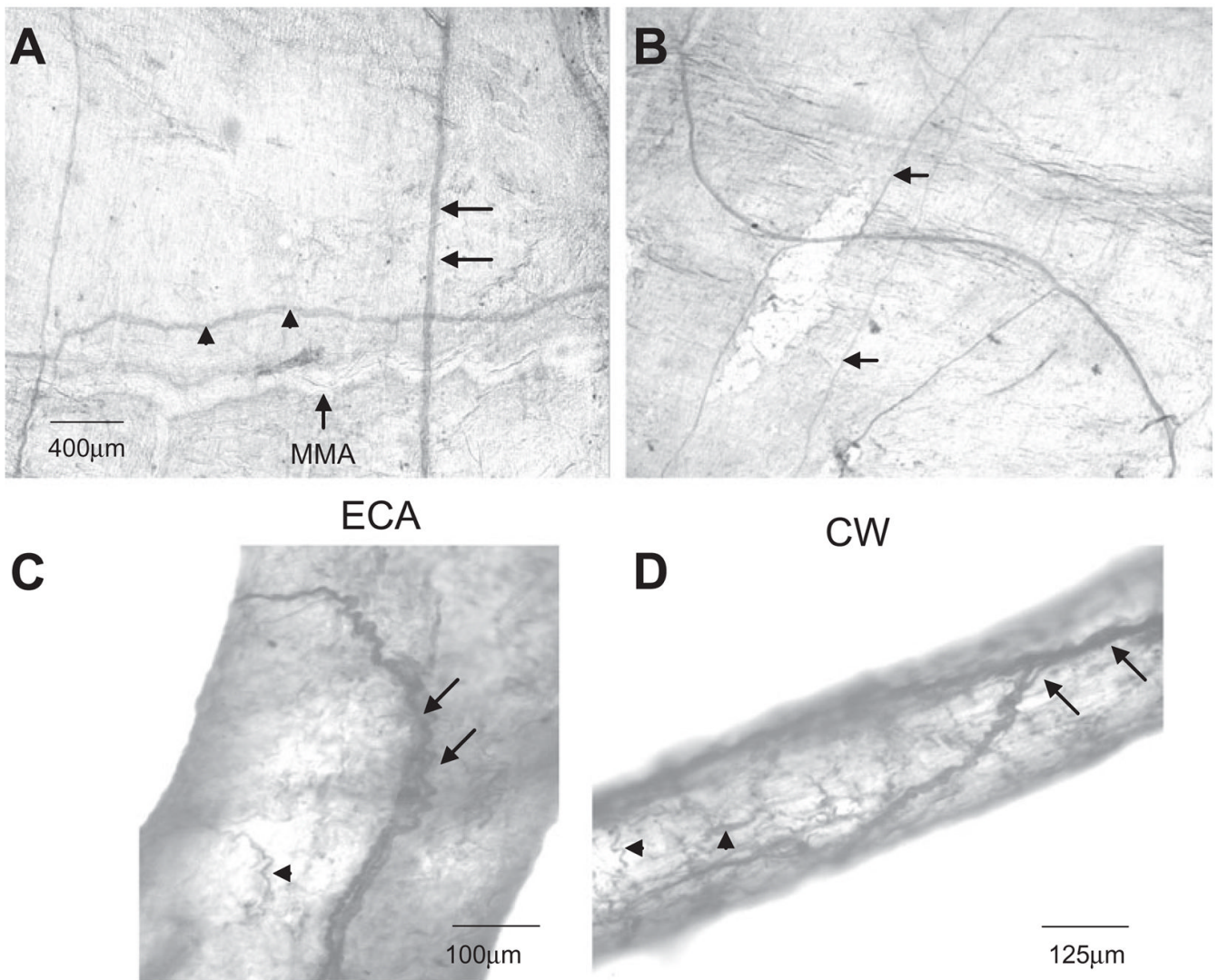


Figure 2. (A) Diaminobenzidine immunohistochemistry of 5HT_{1D}R in cerebrovascular tissues. 5HT_{1D}R LI is found in nerve fibres innervating dura mater and run parallel (arrowheads) and perpendicular (arrow) to the middle meningeal artery (MMA). (B) There is staining of both larger nerve trunks and smaller fibres (arrow) in the dura. 5HT_{1D}R LI is found in nerve fibres innervating the external carotid arteries (C) and branches of the circle of Willis (D) also. There appears to be staining of fine terminal nerve fibres (arrowheads).

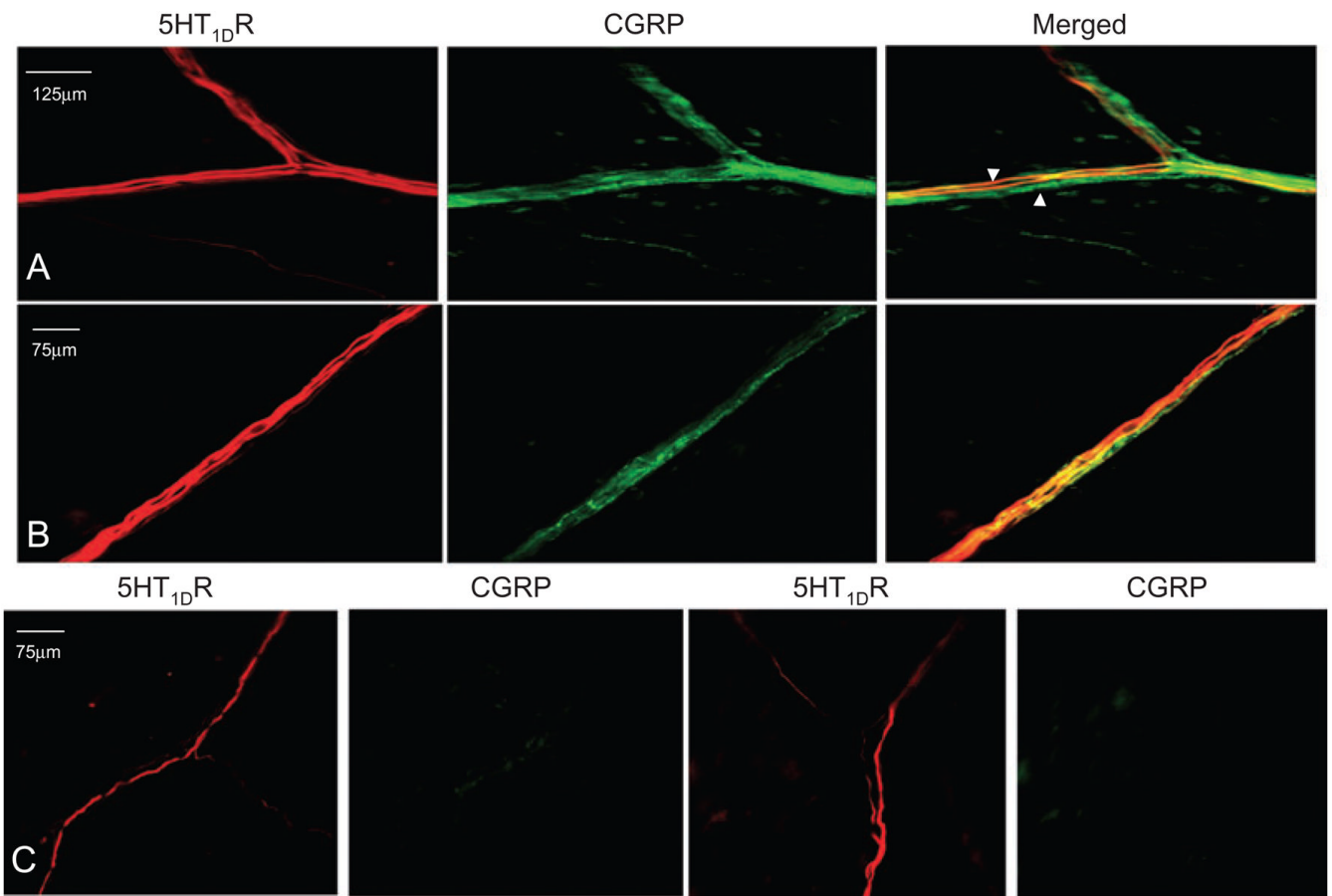


Figure 3.

5HT_{1D}R LI was detected in both peptidergic and non-peptidergic fibres in the dura mater. (A,B) Examples of fibres in which both 5HT_{1D}R LI and calcitonin gene-related peptide (CGRP) LI were detected. There are also CGRP LI fibres that do not overlap with 5HT_{1D}R LI (arrowhead). (C) Examples of fibres in the dura mater in which only 5HT_{1D}R LI was detected.

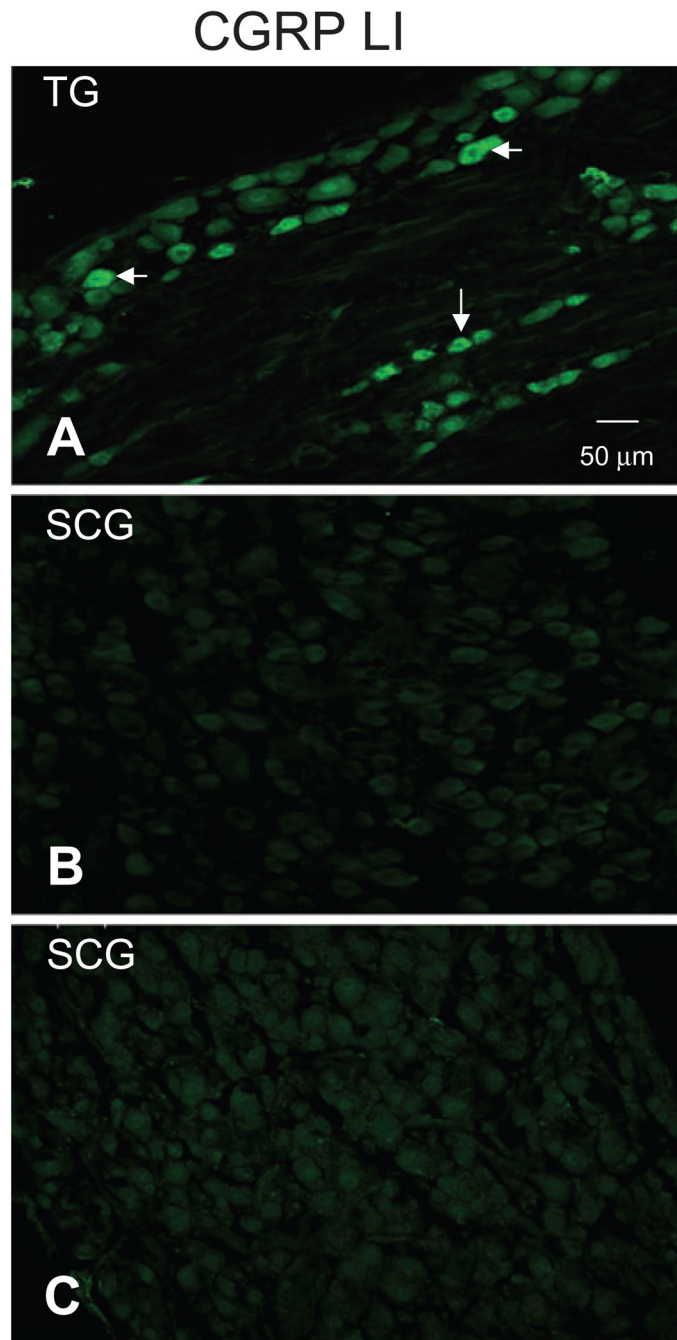


Figure 4. Calcitonin gene-related peptide (CGRP) LI was not detected in rat superior cervical ganglion (SCG). Sections of trigeminal ganglia (TG) (A) and SCG (B) from the same rat were probed in parallel for the presence of CGRP LI. Whereas CGRP-LI was present in a subpopulation of small- and medium-diameter neurons in the TG (arrowheads), CGRP-LI was undetectable in SCG neurons. (C) Omission of primary antibody resulted in a pattern of staining similar to that observed in B.

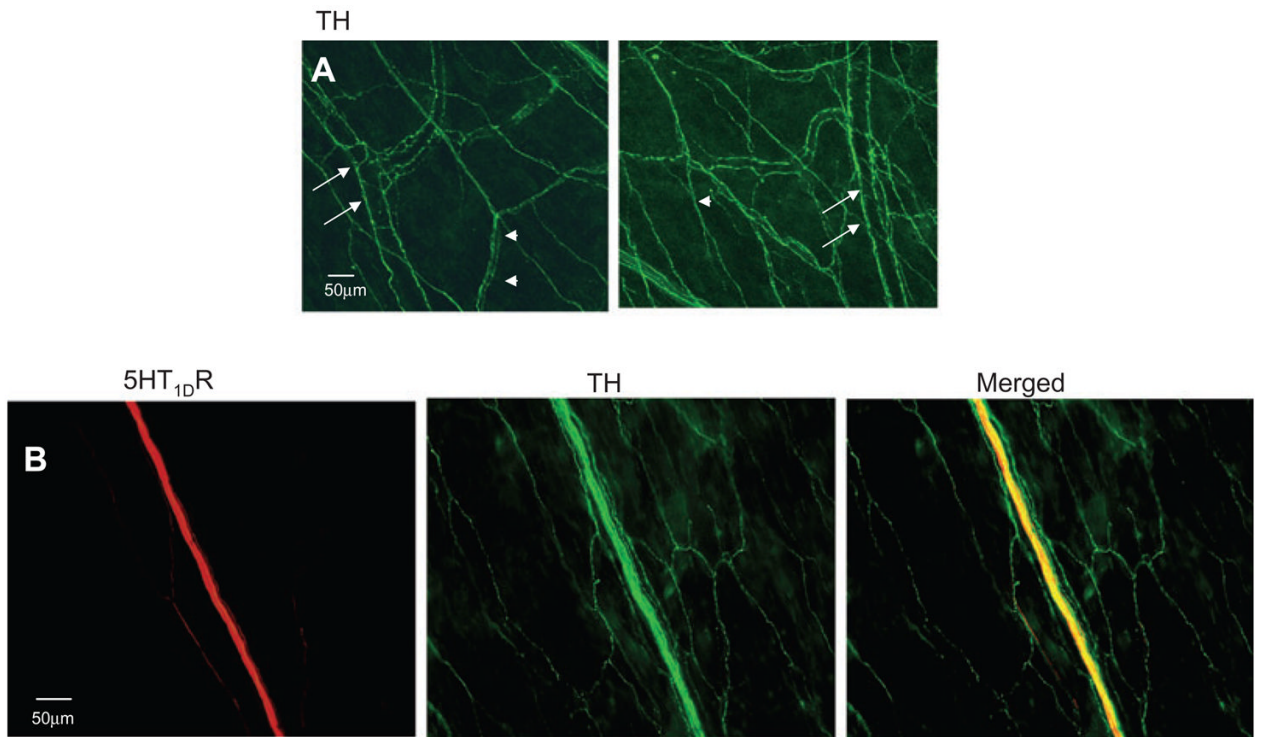


Figure 5. 5HT_{1D}R LI was detected in fibres with tyrosine hydroxylase (TH) LI in the dura. (A) TH LI reveals dense sympathetic postganglionic innervation of the dura mater. TH LI appeared in close proximity to meningeal arteries (arrows) and in the parenchyma of the dura (arrows). (B) Example of fibres in which both 5HT_{1D}R LI and TH LI were detected in the dura.

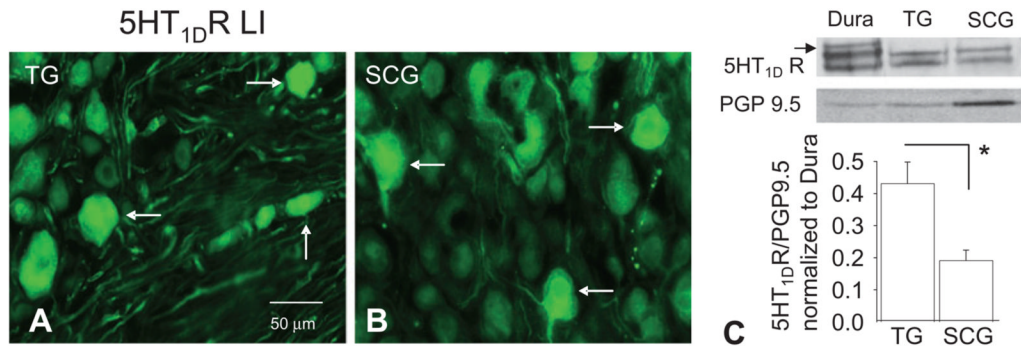


Figure 6. 5HT_{1D}R LI (arrows) was present in subpopulations of neurons in trigeminal ganglia (TG) (A) and superior cervical ganglion (SCG) (B). (C) Top panel: Western blot analysis of 5HT_{1D}R LI in TG and SCG protein: blot is from tissue obtained from a single rat. The high-molecular-weight band present in the dura (arrow) was present in neither TG nor SCG. Bottom panel: Pooled data ($n = 5$) indicate that relative levels of 5HT_{1D}R are greater in TG than in SCG. * $P \leq 0.05$.

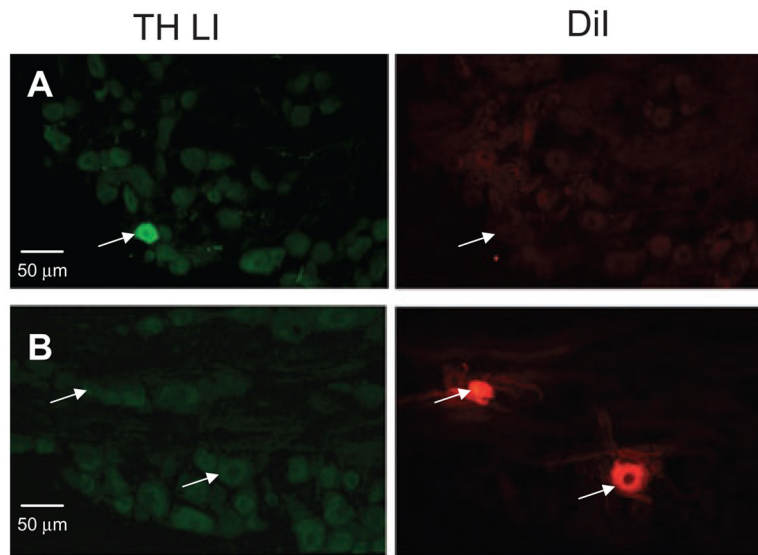


Figure 7. Tyrosine hydroxylase (TH) LI was present in trigeminal ganglia (TG), but not in dural afferents. (A) TH LI was present in a small subpopulation of TG neurons (right panel). None of the TG neurons with TH LI was retrogradely labelled from the dura (middle panel). (B) TH LI was undetectable in TG neurons retrogradely labelled from the dura.